

# Numerical study of the Kardar-Parisi-Zhang equation

Vladimir G. Miranda<sup>a)</sup> and Fábio D. A. Aarão Reis<sup>b)</sup> \*

*Instituto de Física, Universidade Federal Fluminense,  
Avenida Litorânea s/n, 24210-340 Niterói RJ, Brazil*

(Dated: May 31, 2018)

## Abstract

We integrate numerically the Kardar-Parisi-Zhang (KPZ) equation in  $1+1$  and  $2+1$  dimensions using an Euler discretization scheme and the replacement of  $(\nabla h)^2$  by exponentially decreasing functions of that quantity to suppress instabilities. When applied to the equation in  $1+1$  dimensions, the method of instability control provides values of scaling amplitudes consistent with exactly known results, in contrast to the deviations generated by the original scheme. In  $2+1$  dimensions, we spanned a range of the model parameters where transients with Edwards-Wilkinson or random growth are not observed, in box sizes  $8 \leq L \leq 128$ . We obtain roughness exponent  $0.37 \leq \alpha \leq 0.40$  and steady state height distributions with skewness  $S = 0.25 \pm 0.01$  and kurtosis  $Q = 0.15 \pm 0.1$ . These estimates are obtained after extrapolations to the large  $L$  limit, which is necessary due to significant finite-size effects in the estimates of effective exponents and height distributions. On the other hand, the steady state roughness distributions show weak scaling corrections and evidence of stretched exponential tails. These results confirm previous estimates from lattice models, showing their reliability as representatives of the KPZ class.

PACS numbers: 05.40.-a, 05.45.-a, 68.35.Ct, 81.15.Aa

---

\* a) Email address: vladimir@if.uff.br

b) Email address: reis@if.uff.br (corresponding author)

## I. INTRODUCTION

Nearly two decades ago, the Kardar-Parisi-Zhang (KPZ) equation

$$\frac{\partial h}{\partial t} = \nu_2 \nabla^2 h + \lambda_2 (\nabla h)^2 + \eta(\vec{x}, t). \quad (1)$$

was proposed as a hydrodynamic description of interface growth [1]. In Eq. (1),  $h$  is the interface height at position  $\vec{x}$  and time  $t$ , the linear term represents the effect of surface tension, the nonlinear term accounts for an excess velocity due to local slopes and  $\eta$  is a Gaussian noise with zero mean and co-variance  $\langle \eta(\vec{x}, t) \eta(\vec{x}', t') \rangle = D \delta^d(\vec{x} - \vec{x}') \delta(t - t')$ , where  $D$  is constant and  $d$  is the dimension of the substrate. Several applications of the KPZ equation are catalogued in Refs. [2, 3, 4] and recent examples in  $d = 1$  and  $d = 2$  are presented in Refs. [5, 6]. These applications and the intrinsic interest as a non-equilibrium statistical mechanical model motivated an intense theoretical study of its properties and of properties of lattice models in the KPZ class, i. e. models which obey the KPZ equation in the continuum limit (long times, large sizes).

Many properties of KPZ systems in  $d = 1$  are known because the steady state height distribution for periodic boundaries is the same of the Edwards-Wilkinson equation (the case  $\lambda = 0$  - EW) [7]. This result and the Galilean invariance property provide the exact values of the scaling exponents of the average surface roughness [1, 2]. The full height distributions for other boundary conditions in  $d = 1$  are also known [5, 8], but controversies on the universality of correlation functions exist [9] and are subject of current work [10].

On the other hand, a small number of exact results are known in the most important case for applications to real systems, which is  $d = 2$ . Exponents estimates were obtained in  $d \geq 2$  from some analytical approaches [11, 12, 13, 14], but their predictions usually deviate from accurate numerical results of lattice models [15, 16, 17]. Height and roughness distributions were also calculated numerically [15, 16, 17, 18, 19, 20] because they may be useful for comparison with real systems data and for additional tests of the analytical predictions. However, the accurate numerical data currently available were obtained only from two or three lattice models, such as the restricted solid-on-solid (RSOS) model [21], because those works aim at reducing scaling corrections to improve the accuracy of the final estimates. Consequently, no systematic variation of the parameters of the KPZ equation can be performed in such works (although the parameters of the KPZ equation associated to each lattice model may be determined by inverse methods [22, 23]).

It is certainly desirable that the universality of the above mentioned quantities is also tested with the KPZ equation itself with a suitable variation of its coefficients. Indeed, the integration of the KPZ equation was already performed by several authors [24, 25, 26, 27, 28, 29, 30, 31]. However, they usually focus on the calculation of scaling exponents (which typically have lower accuracy than the discrete models data). Giada et al [29] discussed the relevance of other quantities to characterize KPZ scaling, such as the skewness of height distributions, but they did not determine their universal values. The most recent work on the subject seems to be that of Ma et al [30], which suggests exponent values very different from the previous ones.

The aim of this work is to fill that gap by analyzing numerical results for height and roughness distributions in the steady state of the KPZ equation with several sets of coefficients. Estimates of roughness exponents will also be provided here. Our results confirm the universality of these quantities, with the values previously suggested by lattice model simulation. Of particular relevance is to confirm that the roughness distribution has a stretched exponential tail, which reflects the non-Gaussian behavior of the interface. We also show that the calculation of reliable roughness exponents and of dimensionless amplitude ratios characterizing the height distribution has to account for the presence of finite-size corrections, which are much smaller in the scaling of roughness distributions. These features resemble those found in lattice models and show that the finite-size corrections are not artifacts of those models.

We will adopt an Euler scheme for integration. The main problem of using a simple version of this method [27] is the onset of instabilities in the growing interface at long times, as indicated by the divergence of the height at a certain position [32, 33]. However, we will control this instability by replacing the square gradient in Eq. (1) by an exponentially decreasing function of this quantity, as suggested by Dasgupta et al [32, 33]. Another previously reported problem of the simple Euler scheme is the anomalous value of the amplitude of steady state roughness scaling in  $d = 1$  [34]. However, we will show that this anomaly also disappears with the introduction of the exponentially decreasing nonlinear term, without needing special discretization schemes. The use of a framework which avoids different types of anomaly in the integration of the KPZ equation is certainly relevant and is a subject of current interest even for studies in  $d = 1$  [31].

The rest of this work is organized as follows. In Sec. II we present the quantities of

interest of this work. In Sec. III we present the integration scheme and show results for the one-dimensional case, where exact solutions are known. In Sec. IV we present the results in  $d = 2$ . In Sec. V we summarize our results and present our conclusions.

## II. THE QUANTITIES OF INTEREST

The simplest quantitative characteristic of a given interface is its roughness [2], also called the interface width, defined as the rms fluctuation of the height around the average position. The squared roughness,  $w_2 \equiv \overline{h^2} - \bar{h}^2$ , is usually averaged over different configurations, and its scaling on time and length is used to describe non-equilibrium growth processes. For short times, the average roughness scales as

$$\langle w_2 \rangle \sim Bt^{2\beta}, \quad (2)$$

where  $\beta$  called the growth exponent and  $B$  is a scaling amplitude. For long times, in a finite system of size  $L$ , a steady state is attained, with the average width saturating at

$$\langle w_2 \rangle_{sat} \approx AL^{2\alpha}, \quad (3)$$

where  $\alpha$  is called the roughness exponent and  $A$  is another scaling amplitude.

The exponents  $\alpha$  and  $\beta$ , as well as the dynamical exponent  $z = \alpha/\beta$ , are the quantities most frequently used to characterize a given universality class of growth. For the KPZ class, Galilean invariance leads to the additional exact relation  $\alpha + z = 2$  [1, 2].

A better description of the interface is provided by the full height distribution, measured relatively to the average height. The moments of the steady state height distribution,

$$W_n \equiv \left\langle \overline{(h - \bar{h})^n} \right\rangle, \quad (4)$$

may be used to characterize it. Numerical works usually consider some dimensionless amplitude ratios for this purpose [18, 19], particularly if finite-size effects in the scaled height distributions are found and extrapolations to infinite system size are necessary [15, 17]. The lowest order ratios are the skewness

$$S \equiv \frac{W_3}{W_2^{3/2}}, \quad (5)$$

which is related to the asymmetry of the distribution, and the kurtosis

$$Q \equiv \frac{W_4}{W_2^2} - 3, \quad (6)$$

which is related to the weight of the tails of the distribution relatively to a Gaussian.

Recent works suggest that the statistics of global quantities may be more useful for characterizing an interface growth problem. The main quantity of interest is certainly the squared roughness [35, 36, 37], whose probability of being in the range  $[w_2, w_2 + dw_2]$  will be denoted by  $P_w(w_2)dw_2$ . The probability density  $P_w$  is expected to scale as

$$P_w(w_2) = \frac{1}{\sigma} \Psi\left(\frac{w_2 - \langle w_2 \rangle}{\sigma}\right), \quad (7)$$

where  $\sigma \equiv \sqrt{\langle w_2^2 \rangle - \langle w_2 \rangle^2}$  is the root-mean-square deviation. Compared to other scaling forms for  $P_w(w_2)$ , Eq. (7) has the advantage of being less sensitive to finite-size effects and, consequently, more useful in data collapse work [38]. Anyway, comparison of dimensionless ratios such as the skewness and the kurtosis of roughness distributions are important quantitative tests.

### III. INTEGRATION METHOD AND RESULTS IN $d = 1$

The usual discretization of Eq. (1) follows the lines of Ref. [27], which gives in  $d = 1$

$$h(t + \Delta t) - h(t) = \frac{\Delta t}{(\Delta x)^2} \left\{ \nu [h(x-1) - 2h(x) + h(x+1)] + \frac{1}{8} \lambda [h(x+1) - h(x-1)]^2 \right\} + \sigma \sqrt{12\Delta t} R(t). \quad (8)$$

In Eq. (8),  $\sigma \equiv \sqrt{2D/(\Delta x)^d}$  and  $R$  is a random number taken from a uniform distribution in the interval  $[-0.5, +0.5]$ . In  $2 + 1$  dimensions, similar contributions of the  $y$  direction to the laplacian and to the square gradient are added to the right side of Eq. (8).

The spatial step  $\Delta x = 1$  can be used without loss of generality, since decreasing  $\Delta x$  would be equivalent to decreasing the parameter  $\lambda$  in Eq. (1) [26, 27, 34]. Here, the lattice size  $L$  used in the numerical integration has maximum values  $L = 128$  both in  $d = 1$  and  $d = 2$ . On the other hand,  $\Delta t$  has to be sufficiently small to provide accurate results. One ensures that a certain value of  $\Delta t$  is suitable for a certain set of parameters by verifying that further decreasing of its value does not change the results. As usual, we adopt  $\nu$ ,  $\sigma$  and  $g \equiv \lambda^2 D / \nu^3$  as free parameters in the discretized equation [27].

Although Eq. (8) provides reliable estimates of growth and roughness exponents in  $d = 1$  with relatively small system sizes, this discretization procedure has some problems. First, Lam and Shin [34] showed that it provides incorrect values of the scaling amplitude  $A$  in

Eq. (3), which depends on  $\nu$  and  $D$ . The deviation from the expected exact value of  $A$  is observed even after extrapolation to  $L \rightarrow \infty$ . The same authors proposed an improved discretization in  $1 + 1$  dimensions [39], but it was based on particular properties of the KPZ equation in that dimension and, consequently, cannot be extended to the main case of interest here ( $2 + 1$  dimensions). Secondly, Dasgupta et al [32, 33] showed that the above discretization generates instabilities in the interface, in which isolated pillars or grooves grow in time on an otherwise flat interface. In  $d = 1$ , these instabilities typically appear for large values of  $g$  and for sufficiently long integration times and/or lattice sizes. Moreover, these instabilities are not consequence of unsuitably large time steps, but an intrinsic feature of the discretization of the KPZ and other nonlinear equations [33].

In order to solve the second problem (the instabilities), here we adopt the scheme proposed in Refs. [32, 33], in which  $(\nabla h)^2$  in the KPZ equation is replaced by  $f((\nabla h)^2)$ , where

$$f(x) \equiv (1 - e^{-cx})/c, \quad (9)$$

with  $c$  being an adjustable parameter. This method avoids that large local height differences lead to very large growth rates, which is the origin of the instabilities [33]. The new discretized equation is obtained along the same lines of Eq. (8), i. e. the square gradient is estimated from the nearest neighbor height differences in all spatial directions and the corresponding value of  $f((\nabla h)^2)$  is calculated from it.

Notice that the replacement of  $(\nabla h)^2$  by  $f((\nabla h)^2)$  corresponds to the introduction of an infinite series of higher-order nonlinear terms in the KPZ equation. Their introduction does not change the scaling exponents and other universal quantities [2].

Figs. 1a and 1b illustrate the growth of an instability when Eq. (8) is used with  $\nu = 1$ ,  $D = 1$  and  $g = 48$ , in a one-dimensional interface with  $L = 500$ , when time increases from 55.5 to 55.8 ( $\Delta t = 0.05$  there). This instability disappears after the replacement of  $(\nabla h)^2$  by  $f((\nabla h)^2)$  with  $c = 1$  and integration with the same parameters. It is important to stress that  $c$  cannot be very large, otherwise nonlinear effects become very weak and a long transient with EW scaling is found (similarly to what happens in lattice models - see e. g. Ref. [40]). Anyway, in all our simulations in  $d = 1$  and  $d = 2$  using  $c$  not too small, no instability was observed in the growth regimes nor in the (very long) steady states.

During the integration of Eq. (8) with and without the instability control, we also analyzed the first problem mentioned above. Restricting the comparison to situations where

no instability is observed (small  $\lambda$  and small lattice sizes), we measured the amplitude

$$A' \equiv 12 * \langle w_2 \rangle_{sat} / L \quad (10)$$

in the steady states. It is expected that  $A' \rightarrow 1$  as  $L \rightarrow \infty$  ( $\alpha = 1/2$  in  $d = 1$ ) [41].

The finite-size estimates of  $A'$  are shown in Fig. 2. With the simple Euler method (Eq. 8), the numerical value of  $A'$  converges to a value close to 0.85, as reported in Ref. [34]. However, this discrepancy is also eliminated with the new discretization, i. e. with  $f((\nabla h)^2)$  replacing  $(\nabla h)^2$ . Fig. 2 clearly shows that the finite-size estimates of  $A'$  are consistent with an asymptotic value  $A' = 1$  within small error bars.

Thus, the method to control instabilities also solves another problem related to the discretization of the KPZ equation, which is the incorrect estimation of scaling amplitudes in the regime where the original discretization [Eq. (8)] seems to be stable. This advances over most previous works on the subject because, as far as we know, they analyzed those anomalies separately. The only exception seems to be a recent work which compared the original Euler scheme and pseudospectral methods [31], which shows that the latter avoids instabilities in  $d = 1$  and provides the correct value of the amplitude  $A'$  [31]. One difference from the present approach is that here the KPZ equation was modified in real space. Another important difference is that instability suppression with the pseudospectral method requires small time steps such as  $\Delta t \sim 10^{-3}$ , while with  $\Delta t \sim 10^{-2}$  they have a non-negligible chance to appear in  $d = 1$  [31]. On the other hand, here we obtained satisfactory results with  $\Delta t > 10^{-2}$  in  $d = 1$  and  $d = 2$ .

#### IV. RESULTS IN $d = 2$

Here we consider four sets of values of the model parameters, with  $\nu = 0.5$  and  $\sigma = 0.1$  kept fixed and varying  $g \equiv \lambda^2 D / \nu^3$ , which corresponds to different intensities of the nonlinearity. Suitable values of the constant  $c$  were chosen to avoid instabilities, typically increasing with  $g$ . The values of the parameters used in each data set are shown in Table I, in increasing order of nonlinearity from A to D.

Our aim is to span a reasonable region of the parameter space, but both very small and very large  $g$  are difficult to work with. Small nonlinearities must be avoided because the results would show long transients with EW scaling [40] or with random growth. In

such cases, KPZ scaling would only be observed in very large box sizes, where it is difficult to generate a large number of independent steady state configurations due to the large saturation times ( $z \approx 1.6$  [17]). On the other hand, working with very high  $g$  is not good because the large values of  $c$  introduce large irrelevant terms in the KPZ equation which play a role in the finite-size scaling, possibly showing crossovers from other dynamics.

We worked with five different box sizes, ranging from  $L = 8$  to  $L = 128$ . The time step here was  $\Delta t = 0.04$ , and  $\Delta x = \Delta y = 1$ , for all sets of the parameters. Maximum simulation times ranged from  $10^3$  for the smaller sizes to  $10^4$  for the largest one. These times are much larger than the saturation times, so that long steady state regimes were obtained in each realization. The total number of realizations for each set of model parameters was  $2 \times 10^3$  for  $8 \leq L \leq 64$  and  $10^3$  for  $L = 128$ .

Finite-size estimates of the roughness exponents were calculated as

$$\alpha(L) \equiv \frac{1}{2} \frac{\ln [\langle w_2 \rangle(L) / \langle w_2 \rangle(L/2)]}{\ln 2}. \quad (11)$$

These effective exponents are expected to converge to the dominant, asymptotic exponent  $\alpha$  as  $L \rightarrow \infty$ . However, work on discrete models and with growth equations show that Eq. (3) may have correction terms, which leads to an  $L$ -dependence of  $\alpha(L)$ .

In Fig. 3 we show  $\alpha(L)$  versus  $1/L$  for all sets of parameters of the KPZ equation. Since we were not able to obtain results in large box sizes in a reasonable computation time, the estimates of  $\alpha$  are not so accurate as those calculated from lattice models [15, 17]. For small nonlinearity (set A), we note a significant size dependence of  $\alpha(L)$ , thus the extrapolation for  $L \rightarrow \infty$  has lower accuracy than that for sets B and C. The trend of the data for set D (high nonlinearity) is different from the other sets, probably due to a much more complex crossover to the asymptotic scaling.

For the above reasons, our extrapolation of the effective exponents is mainly based on the behavior of the data sets B and C, which give  $0.37 \leq \alpha \leq 0.40$  (we adopted the same extrapolation methods of Ref. [17] for all sets). These values agree with the best current estimate  $\alpha \approx 0.39$  from the lattice models [15, 17], which suggests that those models actually work as representatives of the KPZ class. The trend of all data sets in Fig. 3 suggest that the simple rational guess  $\alpha = 2/5$  (proposed in Ref. [11]) is not valid, although it is not discarded from the final error bar.

The former estimates of  $\alpha$  from integration of the KPZ equation were as low as 0.18 [24]

and 0.24 [25], but subsequent works provided estimates closer to 0.4 [26, 28]. The exponent  $\beta = 0.24$  obtained by Moser et al [27] is consistent with the latter values (using  $\alpha + z = 2$ ). A recent work with a pseudospectral method provided estimates ranging from 0.38 to 0.40 (central estimates) from the scaling of different quantities. Thus, it is surprising that the most recent numerical solution of the KPZ equation [30] suggests that  $z = 2$  and that the exact result  $\alpha + z = 2$  is not obeyed. We believe that this discrepancy is caused by the use of very low nonlinearities in Ref. [30], which leads to a long EW regime. In this case, KPZ scaling can only be detected in very large boxes and very long times.

Now we turn to the analysis of the height distributions. Due to finite-size effects, we focus on the scaling of dimensionless amplitude ratios that characterize those distributions. Thus, in Figs. 4a and 4b we show the skewness and the kurtosis of the height distribution, respectively, as a function of  $1/L$ .

Estimates of  $S$  are accurate and consistent with an asymmetry in the distribution, with positive  $S$  meaning sharp peaks and flat valleys (for positive  $\lambda$ ). Since  $S = 0$  for EW growth, a small value of  $S$  is a signature of a crossover from EW to KPZ. This is consistent with the results for  $L = 8$  and  $L = 16$  in Fig. 4a, which show increasing  $S$  for increasing nonlinearity, with  $S \approx 0.05$  for the smallest  $g$  (set A).

Universality of  $S$  in the continuum limit is suggested by extrapolation of the results of all sets to  $1/L \rightarrow 0$ . The intersections of at least two extrapolated values, with the corresponding error bars, lead to  $S = 0.25 \pm 0.01$ . The central estimate is slightly below the value  $|S| = 0.26 \pm 0.01$  obtained in the discrete models [15, 17], suggesting that  $|S| = 0.25$  up to two decimal places. Here we recall that negative  $\lambda$  would lead to negative  $S$ , but with an universal  $|S|$ , as discussed in Ref. [17].

The estimates of the kurtosis  $Q$  are less accurate, mainly for the largest sizes, but extrapolations indicate a universal positive  $Q$ . Intersections of at least two extrapolated values lead to  $Q = 0.15 \pm 0.1$ , which is also consistent with the estimate  $Q = 0.134 \pm 0.015$  obtained in discrete models [15, 17].

Now we discuss the roughness distribution scaling. In Fig. 5 we show the scaled distributions [using Eq. (7)] for two sets of parameters (C and D) in box size  $L = 128$  and the distribution for the RSOS model in lattice size  $L = 256$  [20]. The excellent agreement of these curves in three decades of the scaled probability density illustrates the universality previously suggested by simulation of discrete models [20]. Comparison of results in  $L = 64$

and  $L = 32$  show that finite-size effects are very small. Quantitative evidence of the agreement is provided by the estimates of their skewness and kurtosis: averaging results for all sets, we obtain  $S = 1.73 \pm 0.04$  and  $Q = 5.6 \pm 1.1$ , which must be compared with lattice models data  $S = 1.70 \pm 0.02$  and  $Q = 5.4 \pm 0.3$  [20]. Here, the largest deviations from the central values are provided by the sets A and D, similarly to the other quantities. However, those deviations are so slight that they cannot be detected by visual inspection of the distributions (see e. g. the data for set D in Fig. 5). Overall averages of  $S$  and  $Q$  are fully consistent with universality of roughness distributions, and the above discussion reinforces the conclusion that they exhibit much smaller corrections to scaling than other quantities.

An important feature of the KPZ roughness distribution is the apparently stretched exponential tail, which is suggested in Fig. 5 by a small upward curvature in the right tail. In order to analyze the tails of our curves, we assume that  $\Psi \equiv \sigma P_L(w_2)$  decays as  $\Psi(x) \sim \exp(-Ax^\gamma)$ , where  $x \equiv \frac{w_2 - \langle w_2 \rangle}{\sigma}$  [see Eq. (7)]. Thus, estimates of the exponent  $\gamma$  can be obtained from

$$\gamma(x) = \frac{\ln \left[ \frac{\ln(\Psi(x))}{\ln(\Psi(x-\Delta))} \right]}{\ln \left[ \frac{x}{x-\Delta} \right]}, \quad (12)$$

with constant  $\Delta$ .

In Fig. 6 we show  $\gamma(x)$  versus  $1/x^2$  for three sets of parameters (B, C and D) and  $L = 64$ , using  $\Delta = 4$  in Eq. (12). This box size was used because fluctuations in the tails of the distributions for  $L = 128$  are much larger. The trend of the data as  $x \rightarrow \infty$  suggests that the tail of the roughness distribution is an stretched exponential with an exponent between  $\gamma = 0.7$  and  $\gamma = 0.9$ . This is consistent with results of lattice models, which give  $\gamma \approx 0.8$ .

## V. CONCLUSION

We solved numerically the KPZ equation in  $1 + 1$  and  $2 + 1$  dimensions with an Euler discretization scheme. The  $1 + 1$ -dimensional case confirms the appearance of instabilities for high nonlinearities and large box sizes. These instabilities are suppressed by replacement of  $(\nabla h)^2$  by a exponentially decreasing function of this quantity in the KPZ equation and subsequent discretization. Moreover, this change leads to consistent estimates of scaling amplitudes, in contrast to the discretization scheme of the original equation. In  $2 + 1$  dimensions, we spanned a reasonable range of the model parameters where crossover effects (i. e. transients with EW growth or random growth) are not observed. We confirmed the

universality of roughness exponents, height distributions and roughness distributions in the steady state, which were previously obtained in discrete models. Estimates of skewness and kurtosis of those distributions were provided in order to show the quantitative agreement with previous results. We also showed evidence that the tails of the roughness distributions are stretched exponentials, which also agrees with discrete model results and suggests the non-Gaussianity of the steady state KPZ interfaces in  $2 + 1$  dimensions.

Our results are not able to improve the accuracy of simulations of discrete models, which is expected for the computational limitations in the work with floating point operations. At first sight, this could seem to diminish the relevance of the present work. However, we stress that the connections between the lattice models and the KPZ equation do not follow from rigorous mathematical proofs, and some models are controversial at this point (e. g. ballistic deposition [42]). Moreover, works on discrete models are not able to vary the parameters of the corresponding KPZ equations in a systematic way; indeed, only two or three of those models provide finite-size data which are clearly consistent with universality (see e. g. Ref. [17]). Thus, confirming results in the context of the KPZ equation itself, with different parameter values, is of great importance. As far as we know, this is the first quantitative discussion on height and roughness distributions obtained from integration of the KPZ equation in  $2 + 1$  dimensions. Those quantities are very useful for a complete characterization of a growth class, particularly due to the effects of scaling corrections in the estimates of exponents.

We also believe that this work can motivate future studies in higher dimensions, where the debate on the existence of a finite upper critical dimension (the dimension where the nonlinearity is always irrelevant) still remains [14, 43], despite the strong numerical evidence against it provided by results of two lattice models [16, 17]. Since such studies would demand an efficient integration scheme to provide the best possible accuracy in reasonable simulation times, one must consider the possible advantages of other approaches, such as the pseudospectral methods [29, 31].

### **Acknowledgments**

The authors thank T. J. Oliveira for helpful discussion. V.G.M. acknowledges support from CNPq and F.D.A.A.R. acknowledges support from CNPq and FAPERJ (Brazilian

agencies).

- 
- [1] M. Kardar, G. Parisi and Y.-C. Zhang, Phys. Rev. Lett. **56**, 889 (1986).
  - [2] A.L. Barabási and H.E. Stanley, *Fractal concepts in surface growth* (Cambridge University Press, Cambridge, England, 1995).
  - [3] J. Krug, Adv. Phys. **46**, 139 (1997).
  - [4] J. Krim and G. Palasantzas, Int. J. Mod. Phys. B **9**, 599 (1995).
  - [5] L. Miettinen, M. Myllys, J. Merikoski, and J. Timonen, Eur. Phys. J. B **46**, 55 (2005).
  - [6] D. Tsamouras, G. Palasantzas, and J. Th. M. de Hosson, Appl. Phys. Lett. **79**, 1801 (2001).
  - [7] S. F. Edwards and D. R. Wilkinson, Proc. R. Soc. London **381**, 17 (1982).
  - [8] M. Prähofer and H. Spohn, Phys. Rev. Lett. **84**, 4882 (2000).
  - [9] E. Katzav and M. Schwartz, Phys. Rev. E **69**, 052603 (2004).
  - [10] S. Bustingorry, J. Stat. Mech.: Theory Exp. P10002 (2007).
  - [11] M. Lässig, Phys. Rev. Lett. **80**, 2366 (1998).
  - [12] F. Colaiori and M. A. Moore, Phys. Rev. Lett. **86**, 3946 (2001).
  - [13] H. C. Fogedby, Physica A **314**, 182 (2002).
  - [14] H. C. Fogedby, Phys. Rev. Lett. **94**, 195702 (2005).
  - [15] E. Marinari, A. Pagnani and G. Parisi, J. Phys. A **33** (2000) 8181.
  - [16] E. Marinari, A. Pagnani, G. Parisi, and Z. Rácz, Phys. Rev. E **65**, 026136 (2002).
  - [17] F. D. A. Aarão Reis, Phys. Rev. E **69**, 021610 (2004).
  - [18] C.-S. Chin and M. den Nijs, Phys. Rev. E **59**, 2633 (1999).
  - [19] Y. Shim and D. P. Landau, Phys. Rev. E **64**, 036110 (2001).
  - [20] F. D. A. Aarão Reis, Phys. Rev. E **72**, 032601 (2005); Physica A **364**, 190 (2006).
  - [21] J. M. Kim and J. M. Kosterlitz, Phys. Rev. Lett. **62** (1989) 2289.
  - [22] C.-H. Lam and L. M. Sander, Phys. Rev. Lett. **71**, 561 (1993).
  - [23] A. Giacometti and M. Rossi, Phys. Rev. E **63**, 046102 (2001).
  - [24] A. Chakrabarti and R. Toral, Phys. Rev. B **40**, 11419 (1989).
  - [25] H. Guo, B. Grossmann and M. Grant, Phys. Rev. Lett. **64**, 1262 (1990).
  - [26] J. G. Amar and F. Family, Phys. Rev. A **41**, 3399 (1990).
  - [27] K. Moser, J. Kertész and D. E. Wolf, Physica A **178**, 215 (1991).

- [28] M. Beccaria and G. Curci, Phys. Rev. E **50**, 4560 (1994).
- [29] L. Giada, A. Giacometti, and M. Rossi, Phys. Rev. E **65**, 036134 (2002).
- [30] K. Ma, J. Jiang, and C. B. Yang, Physica A **378**, 194 (2007).
- [31] R. Gallego, M. Castro and J. M. López, Phys. Rev. E **76**, 051121 (2007).
- [32] C. Dasgupta, S. Das Sarma, and J. M. Kim, Phys. Rev. E **54**, R4552 (1996).
- [33] C. Dasgupta, J. M. Kim, M. Dutta, and S. Das Sarma, Phys. Rev. E **55**, 2235 (1997).
- [34] C.-H. Lam and F. G. Shin, Phys. Rev. E **57**, 6506 (1998).
- [35] G. Foltin, K. Oerding, Z. Rácz, R. L. Workman, and R. K. P. Zia, Phys. Rev. E **50**, R639 (1994).
- [36] Z. Rácz and M. Plischke, Phys. Rev. E **50**, 3530 (1994).
- [37] T. Antal, M. Droz, G. Györgyi, and Z. Rácz, Phys. Rev. E **65**, 046140 (2002).
- [38] T. J. Oliveira and F. D. A. Aarão Reis, Phys. Rev. E **76**, 061601 (2007).
- [39] C.-H. Lam and F. G. Shin, Phys. Rev. E **58**, 5592 (1998).
- [40] T. J. Oliveira, K. Dechoum, J. A. Redinz, and F. D. A. Aarão Reis, Phys. Rev. E **74**, 011604 (2006).
- [41] J. Krug, P. Meakin, and T. Halpin-Healy, Phys. Rev. A **45** 638 (1992).
- [42] E. Katzav and M. Schwartz, Phys. Rev. E **70**, 061608 (2004).
- [43] L. Canet and M. A. Moore, Phys. Rev. Lett. **98**, 200602 (2007).

TABLE I: Nonlinear parameters used in the integration of the KPZ equation in  $2 + 1$  dimensions and the corresponding constant for controlling instabilities. In all cases,  $\nu = 0.5$  and  $\sigma = 0.1$ .

Set	$g$	$c$
A	12	0.1
B	24	0.5
C	48	1.0
D	96	4.0

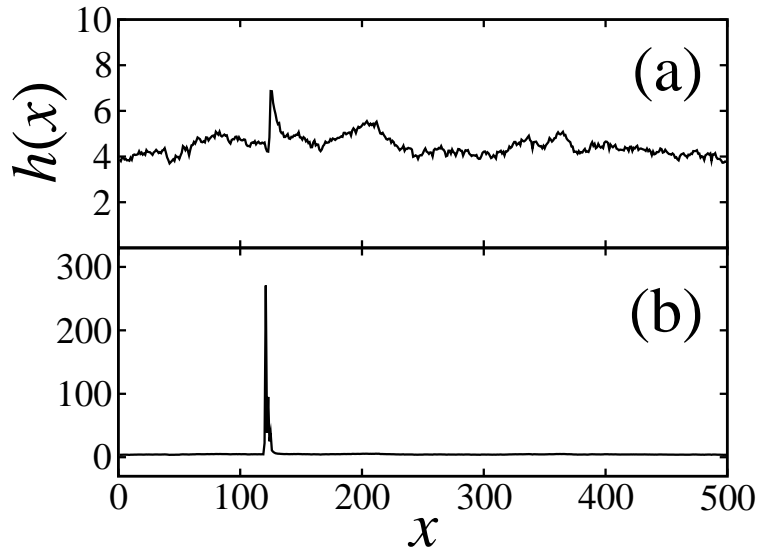


FIG. 1: Interface profiles in  $d = 1$  obtained in the integration of the KPZ equation with Eq. (8) in times (a)  $t = 55.5$  and (b)  $t = 55.8$ . Notice the different vertical scale in (a) and (b) due to the rapid growth of an instability in  $x \approx 120$ .

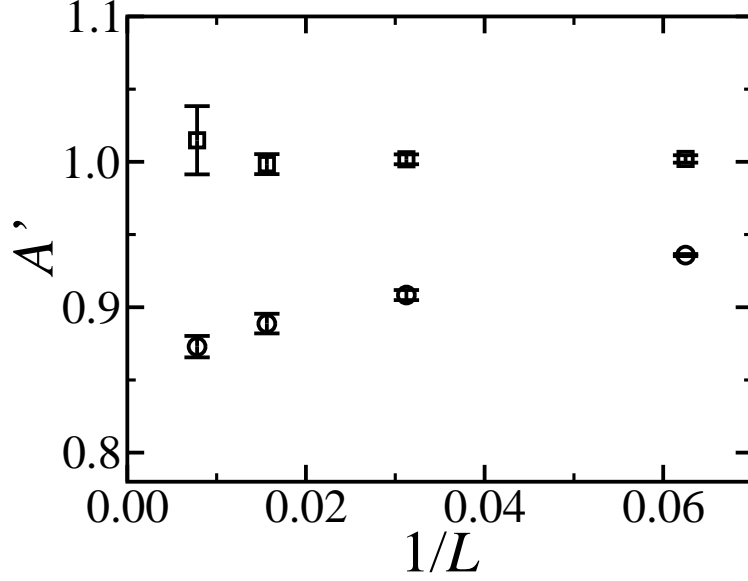


FIG. 2: Amplitude of squared roughness as a function of inverse box size obtained in the integration of the KPZ equation in  $d = 1$  with Eq. (8) (circles) and modified Eq. (8) replacing  $(\nabla h)^2$  by  $f((\nabla h)^2)$  with  $c = 1$  (squares).

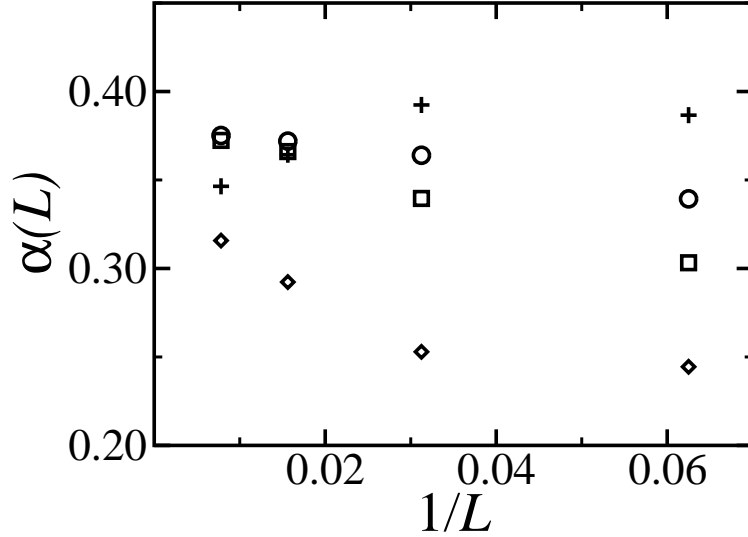


FIG. 3: Effective roughness exponents as a function of inverse box size for KPZ interfaces in  $2 + 1$  dimensions. The symbols correspond to sets A (diamonds), B (squares), C (circles), and D (crosses). For  $L \leq 64$ , error bars are smaller than the size of the data points. For  $L = 128$ , uncertainties in  $\alpha(L)$  are near 0.01.

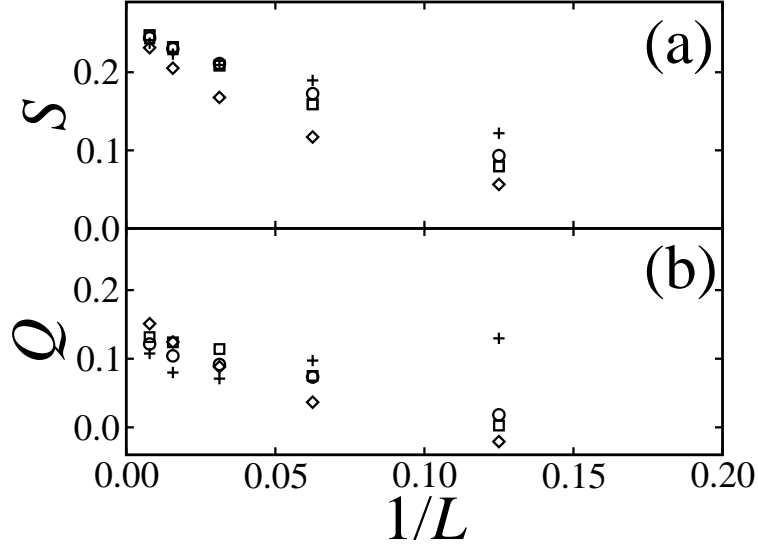


FIG. 4: (a) Skewness and (b) kurtosis of the height distributions of KPZ interfaces in  $2 + 1$  dimensions versus inverse box size. Each symbol corresponds to the same set of Fig. 3. Error bars in  $S$  are of the order of the size of the data points. Uncertainties in  $Q$  are near 0.02 for  $L \leq 64$  and near 0.05 for  $L = 128$ .

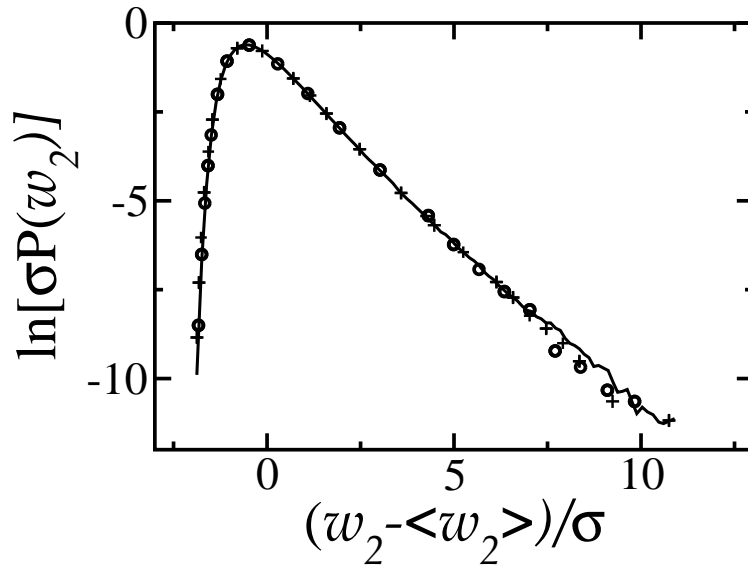


FIG. 5: Scaled roughness distribution of KPZ interfaces in  $2 + 1$  dimensions for sets C and D. Each symbol corresponds to the same set of Fig. 3.

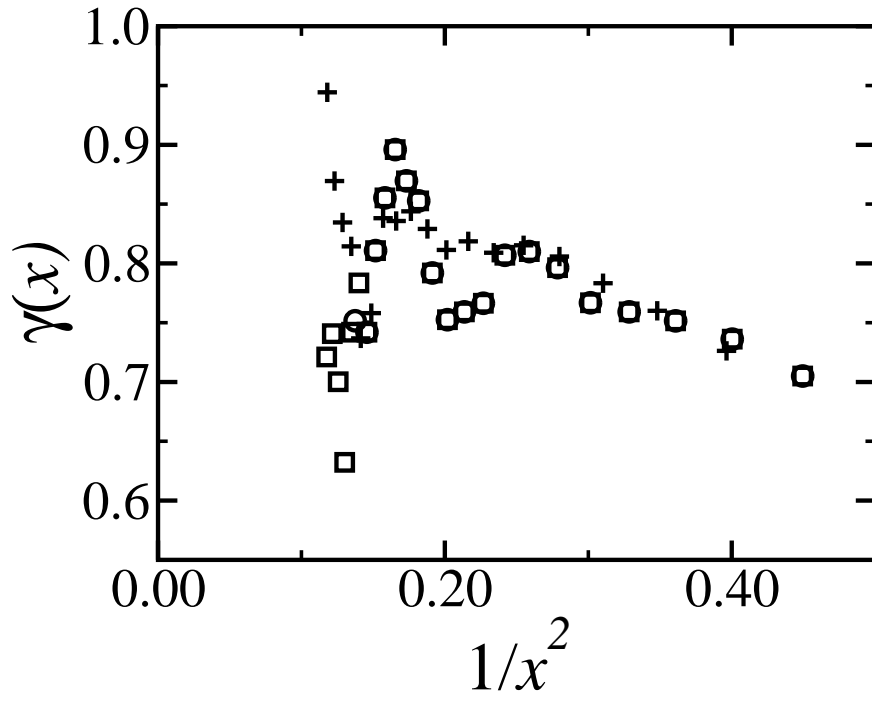


FIG. 6: Effective exponents  $\gamma(x)$  versus  $1/x^2$  of roughness distributions of KPZ interfaces in  $2 + 1$  dimensions. Each symbol corresponds to the same set of Fig. 3.